Geophysical Research Letters

RESEARCH LETTER
10.1029/2025GL117035

Model-Dependent Response of Low Clouds to Arctic Sea-Ice Loss

Ramiro I. Saurral[1,2,3,4], **James A. Screen**[5], **and Francisco J. Doblas-Reyes**[1,6]

[1]Barcelona Supercomputing Center (BSC), Barcelona, Spain, [2]CONICET-Universidad de Buenos Aires. Centro de Investigaciones del Mar y la Atmósfera (CIMA), Buenos Aires, Argentina, [3]Facultad de Ciencias Exactas y Naturales, Departamento de Ciencias de la Atmósfera y los Océanos, Universidad de Buenos Aires, Buenos Aires, Argentina, [4]CNRS-IRD-CONICET-UBA. Instituto Franco-Argentino para el Estudio del Clima y sus Impactos (IRL 3351 IFAECI), Buenos Aires, Argentina, [5]Department of Mathematics and Statistics, University of Exeter, Exeter, UK, [6]Institució Catalana de Recerca i Estudis Avançats (ICREA), Barcelona, Spain

Abstract Clouds play a key role in the climate of the Arctic region. Observational evidence suggests that sea-ice loss fosters increased cloud cover due to enhanced surface turbulent fluxes. Yet, it is not clear whether this mechanism is (well) represented in climate models. In this study we analyze the simulated response of low clouds to sea-ice loss in a set of dedicated numerical model experiments prescribed with changes in sea ice only. We find large discrepancies between models regarding their representation of low cloud responses to identical sea-ice loss. We propose a physical explanation that links biases in simulated present-day surface temperature and stratification to the sign of the low cloud response to sea-ice loss. Our results suggest that mean-state temperature biases need to be reduced in order to narrow uncertainty in the simulated cloud response to sea-ice loss.

Plain Language Summary Sea ice has been quickly melting in the Arctic region during the last decades. This melting is a result of global warming and changes in the regional circulation, but is also controlled by clouds, which modulate the amount of heat that enters and leaves the Earth's surface. In this study, we analyze how a set of climate models represent the relationship between future sea-ice loss and changes in clouds. We find differences in the responses between models, and therefore we look for the physical processes responsible for such disagreements. We find that the main explanation for the observed differences is related to errors in the models to represent the surface temperatures over the Arctic.

Key Points:

- Future sea-ice loss is expected to affect the distribution of high-latitude clouds
- Experiments using different models and forced only by changes in sea-ice cover show large disagreements on cloud response
- Biases in surface temperature are key in shaping the forced response via their influence on the stratification of the lower troposphere

Supporting Information:

Supporting Information may be found in the online version of this article.

Correspondence to:

R. I. Saurral,
ramiro.saurral@bsc.es

Citation:

Saurral, R. I., Screen, J. A., & Doblas-Reyes, F. J. (2025). Model-dependent response of low clouds to Arctic sea-ice loss. *Geophysical Research Letters*, *52*, e2025GL117035. https://doi.org/10.1029/2025GL117035

Received 16 MAY 2025
Accepted 2 SEP 2025

Author Contributions:

Conceptualization: Ramiro I. Saurral, James A. Screen, Francisco J. Doblas-Reyes
Formal analysis: Ramiro I. Saurral, James A. Screen, Francisco J. Doblas-Reyes
Funding acquisition: Ramiro I. Saurral
Investigation: Ramiro I. Saurral, James A. Screen, Francisco J. Doblas-Reyes
Methodology: Ramiro I. Saurral, Francisco J. Doblas-Reyes
Resources: Ramiro I. Saurral
Software: Ramiro I. Saurral
Supervision: James A. Screen, Francisco J. Doblas-Reyes
Visualization: Ramiro I. Saurral
Writing – original draft: Ramiro I. Saurral
Writing – review & editing: James A. Screen, Francisco J. Doblas-Reyes

1. Introduction

The radiative budget of the polar regions is significantly regulated by clouds (Kay et al., 2016 and references therein). Clouds reduce the amount of incoming shortwave and outgoing longwave radiation, controlling the warming/cooling of the surface (e.g., Griesche et al., 2024; Hall, 2004; Maillard et al., 2021; Sledd & L'Ecuyer, 2019), and also modulate the radiative effects of the albedo reduction from sea-ice loss (Goosse et al., 2018; Kay & Gettelman, 2009; Manabe & Stouffer, 1994; Philipp et al., 2020; Sledd & L'Ecuyer, 2021), which is one of the key mechanisms leading to Arctic amplification of surface warming (Screen et al., 2012; Screen & Simmonds, 2010).

The lack of incoming solar radiation combined with the surface heat loss via outgoing longwave radiation during the winter months lead to the formation of a surface temperature inversion layer over most polar regions (Devasthale et al., 2010; Zhang et al., 2011). This layer is usually accompanied by an inversion in specific humidity, which results in high relative humidity values (Tjernström et al., 2004) that lead to the formation of shallow low clouds within the inversion layer (Sedlar & Tjernström, 2009; Wang et al., 2020). Despite the significant relevance of this layer on polar climate, its shallow nature explains the frequent underestimation of its magnitude in climate models (Pithan et al., 2014; Zhang et al., 2021).

Significant advances have been made during the last few years in the characterization of high-latitude clouds, including their role on climate and their interplay with sea ice. Jenkins et al. (2024) concluded that sea-ice loss affects the distribution of clouds via alterations in the lower troposphere stability, which is particularly relevant in winter when strong surface inversions are commonly accompanied by stratiform low clouds (Li et al., 2023). Arouf et al. (2024) concluded that as late-fall sea-ice cover decreases with global warming, the resulting cloud-

driven surface heating increases further over the new open-ocean areas, hindering even more the regeneration of sea ice. Y. Liu and Key (2025) showed that the net response of clouds to sea-ice loss in winter depends on the sea-ice concentration (SIC) during the previous autumn. However, and despite the numerous dedicated campaigns conducted over the Arctic region (e.g., Gryning et al., 2021; Klein and Neggers, 2009; Z. Liu and Schweiger, 2024; Neggers et al., 2012; Philipp et al., 2020; Solomon et al., 2009), our understanding of the comprehensive role of clouds on the polar climate is still limited (Boucher et al., 2013; Griesche et al., 2024; Kay et al., 2016). This knowledge gap may hinder not only a proper validation of model simulations but also the development of trustful climate projections and predictions under sea-ice melting conditions.

The main objective of our study is to quantify the response of low clouds to sea-ice loss in a set of dedicated numerical model experiments developed within the Polar Amplification Model Intercomparison Project (PAMIP; Smith et al., 2019). The PAMIP data set has been extensively used to address the role of sea-ice loss on several weather and climate features (Barnes & Screen, 2015; Cohen et al., 2014; Hay et al., 2023; Screen et al., 2022; Smith et al., 2022; Ye et al., 2024), but not yet clouds. We explore the simulated response of clouds to sea-ice loss in the PAMIP experiments by comparing outputs from present-day experiments against those associated with future reductions in Arctic sea-ice cover. We also identify the physical mechanisms associated with the uneven responses of clouds to sea-ice loss among the models. Our study is centered specifically on low clouds, which are highly susceptible to changes occurring at the surface (Maillard et al., 2021) and represent a major source of uncertainty in numerical models (Tjernström et al., 2008). Our goal is to characterize and understand the low cloud response to sea-ice loss and its sensitivity to model biases.

2. Data and Methods

We use two sets of PAMIP experiments: one representing present-day ("PD") conditions and another one with future ("FUT") sea-ice cover, consistent with a global mean temperature increase of 2°C above pre-industrial levels, but with present-day sea surface temperature (SST). Thus, the only difference between experiments are the prescribed changes in Arctic sea ice. Each experiment includes 100 ensemble members per model of 14-month-long atmosphere-only simulations forced with a seasonal cycle of monthly mean SST and SIC. The first two months are discarded for spin-up, yielding 12-month-long periods for analysis. PD SST and SIC are based on 1979–2008 observations from the Hadley Centre Ice and SST data set (HadISST; Rayner et al., 2003). FUT Arctic SIC is derived from the CMIP5 ensemble mean constrained by observations during the 30-year period in which global mean temperature is 2°C above the pre-industrial period. In areas of sea-ice loss, SSTs are taken from future projections; elsewhere, they match PD values. The response to sea-ice loss is computed as the ensemble-mean difference between FUT and PD. Significance is assessed via a two-sided Student's t-test (p-value = 0.05) followed by a false discovery rate adjustment (Wilks, 2006).

Only four out of the sixteen models participating in the PAMIP had cloud cover outputs available: FGOALS-f3-L, IPSL-CM6A-LR, NorESM2-LM and TaiESM1. Therefore, only these are used. Low-cloud cover (LCC) is defined as the cloud cover maximum amongst all the vertical levels between the surface and 800 hPa. Other variables from PAMIP used here include near-surface temperature, surface sensible and latent heat fluxes (SH and LH, respectively), surface water vapor pressure and the vertical distributions of temperature and moisture. The study focuses on the Northern Hemisphere north of 50°N during boreal winter (December, January and February; DJF) using monthly means. We assess LCC responses to sea-ice loss by computing FUT minus PD ensemble-mean differences in each model individually. Detailed analysis is conducted over the three regions with the largest projected loss of sea ice (Figures 1c and 1d): Hudson Bay (HB), northern Barents-Kara Sea (BK) and Chukchi Sea (CS). The Arctic Ocean (AO) is also examined as its simulated multimodel-mean LCC response is opposite in sign to that in sea-ice loss regions, offering a valuable comparison. Vertical profiles are computed using the MetPy Python package (May et al., 2022).

Although model validation is not our primary goal, ERA5 data (Hersbach et al., 2020) is used to evaluate biases and their influence on cloud responses to sea-ice loss. ERA5 provides winter-mean values of the same variables from 1979 to 2008, matching the PD period.

3. Low Cloud Response to Arctic Sea-Ice Loss

In this section, we quantify the simulated LCC response to sea-ice loss in PAMIP experiments. Figure 1 shows the multi-model ensemble-mean changes in LCC in FUT relative to PD conditions (Figure 1a) along with the spread

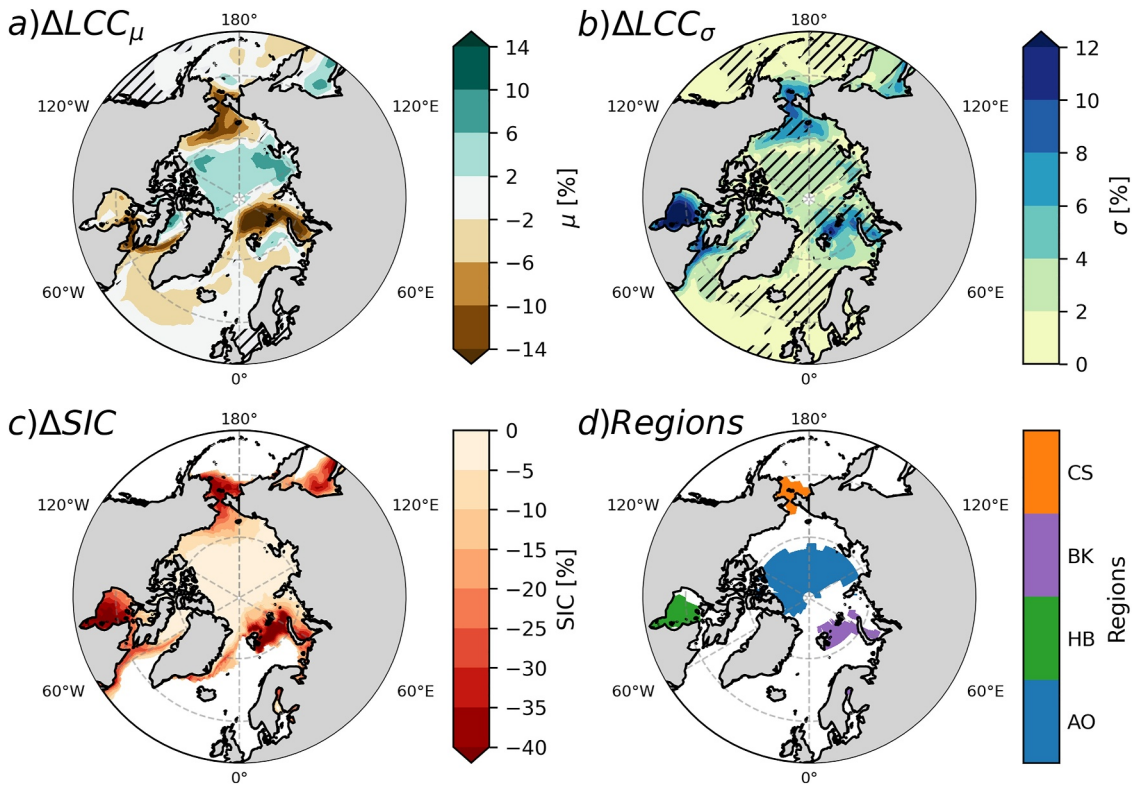

Figure 1. Simulated differences in winter Low-cloud cover (LCC) in FUT relative to PD PAMIP experiments: (a) mean and (b) standard deviation fields across the four climate models. Units are %. (c) Sea-ice concentration differences used to force the PAMIP FUT experiments. Units are % of change relative to PD conditions. (d) Regions used throughout the study: Arctic Region (Arctic Ocean), Hudson Bay, Barents-Kara Sea and Chukchi Sea. Hatching in (a) highlights areas with no significant changes in LCC. Hatching in (b) indicates where all the models coincide in the sign of the simulated changes.

in the response among models (Figure 1b). The multi-model-mean field depicts large differences over areas with significant sea-ice loss (Figures 1a–1c): over BK and CS, sharp reductions in LCC are simulated over and north of the largest reductions in sea ice, whereas over HB variations are also negative but smaller in magnitude. Meanwhile, over AO all models simulate an increase in LCC. The model spread is largest over HB, suggesting that the response of LCC to the same variations in sea-ice cover is model dependent, and smallest over the AO area. In particular, the AO region considered for further analysis was the one north of 70°N and showing in the multi-model mean positive variations in LCC exceeding 2% (Figures 1a–1d).

The LCC responses to sea-ice loss for each model individually are shown in Figures 2a–2d. For reference, the mean fields in PD experiments and in ERA5 are shown in Figure S1 in Supporting Information S1. Hudson Bay stands out as the region with the largest spread in the response, with two models (FGOALS-f3-L and TaiESM1) simulating a decrease, and the two others (IPSL-CM6A-LR and NorESM2-LM) an increase in LCC. Interestingly, models showing the largest reductions in LCC over HB also simulate the largest decreases over the CS region. Over BK, the sign of change is once again model-dependent, even though three out of the four models simulate less LCC under sea-ice loss, while for AO all the models simulate an increase in LCC but of varying magnitudes, from almost 1% (FGOALS-f3-L) to 7.5% (TaiESM1). A comparison of the simulated changes in LCC (Figure 2) with the mean PD fields (Figure S1 in Supporting Information S1) shows that the same models that simulate the largest decreases in cloudiness (i.e., FGOALS-f3-L and TaiESM1) are also those associated with the largest LCC values in the present day across the four regions under analysis. At the same time, the ERA5 mean field (Figure S1e in Supporting Information S1) is, in terms of spatial averages of LCC, more similar to these models than to the ones simulating increased cloud cover.

As a first attempt to explain these disagreements in LCC response we show in Figures 2e–2h the simulated changes in near-surface temperature driven exclusively by sea-ice loss. For reference, the PD mean fields for each model are shown in Figure S2 in Supporting Information S1. The first noticeable feature is the warming found in

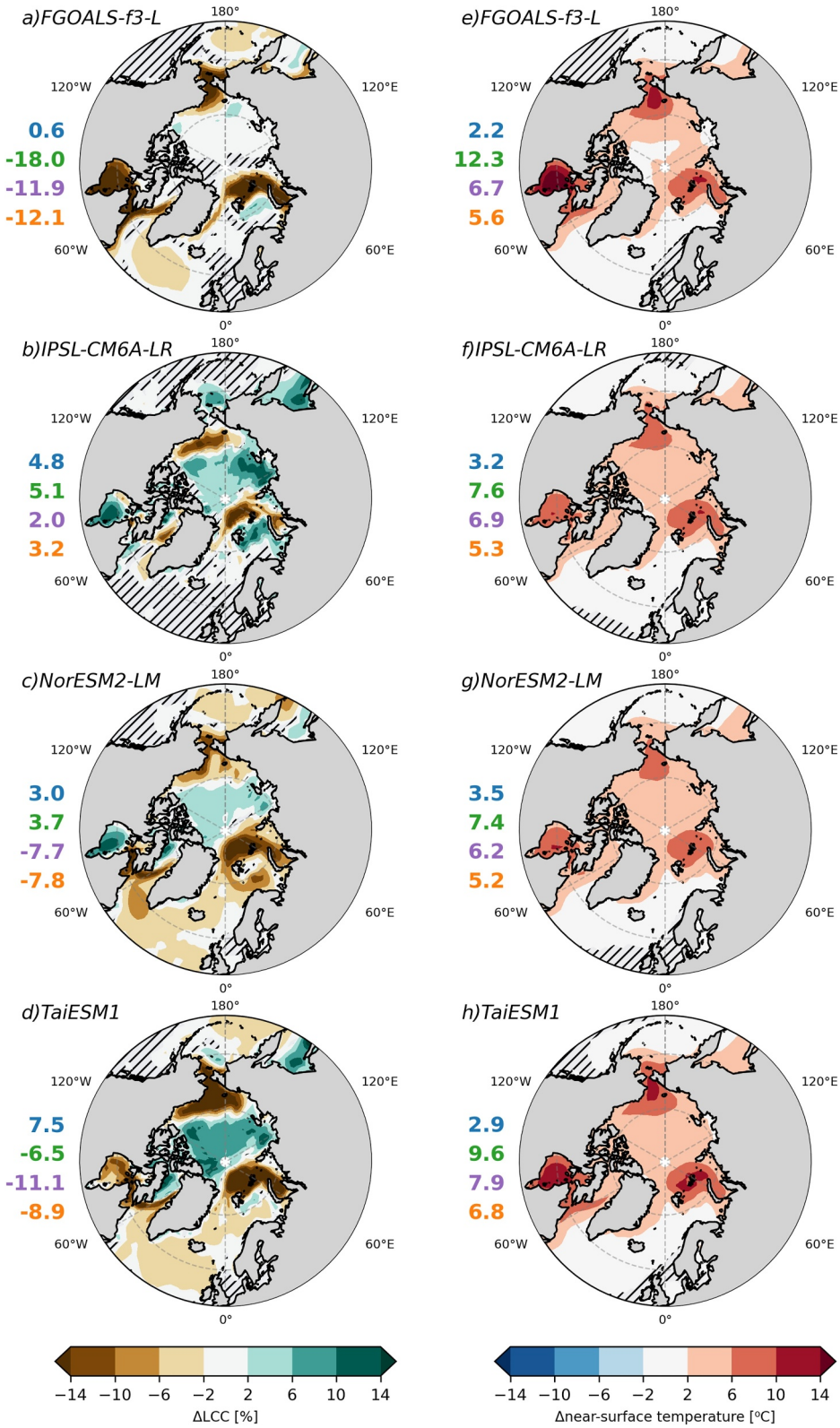

Figure 2. Differences in FUT relative to PD experiments in (left) Low-cloud cover (in %) and (right) near-surface temperature (in °C). Non-significant differences ($p > p_{FDR}$) are highlighted with hatching. The numbers to the left of each figure indicate the mean difference over the four regions (from top to bottom): Arctic Ocean, Hudson Bay, Barents-Kara Sea and Chukchi Sea, using the same color convention as in Figure 1d.

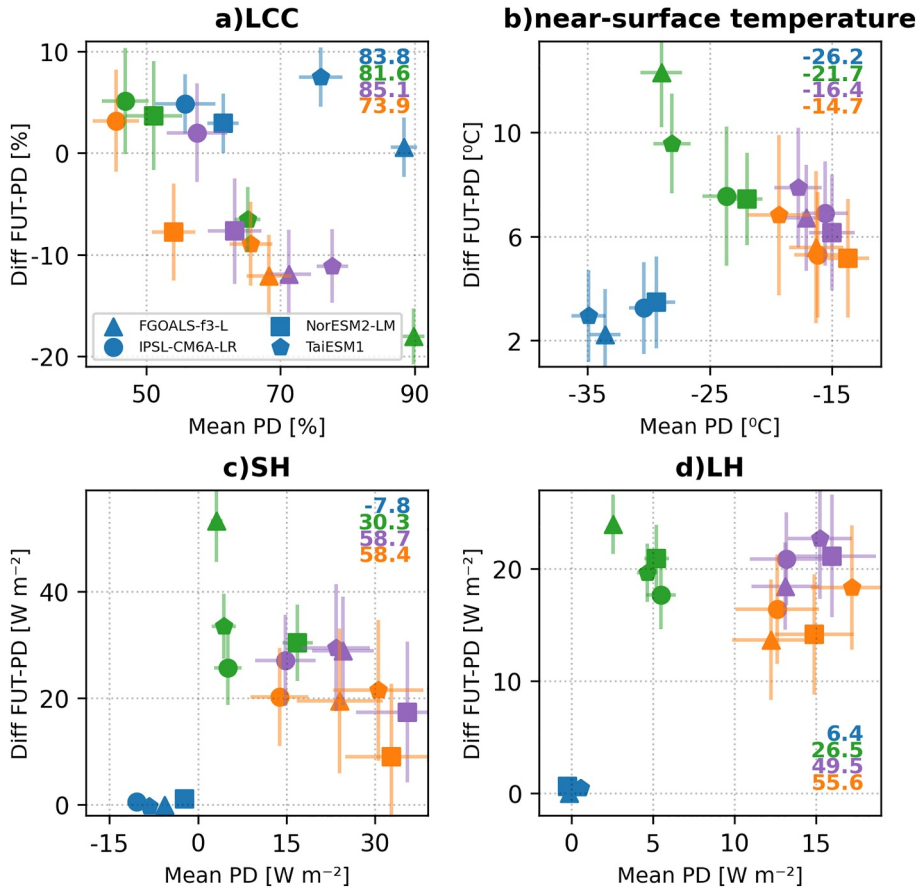

Figure 3. Scatter plots between mean PD values and the differences between FUT and PD of (a) Low-cloud cover (LCC), (b) near-surface temperature, (c) SH and (d) LH in the four GCMs (in symbols; see legend in a) and over the different regions, with the same color convention as before: Arctic Ocean (blue), Hudson Bay (green), BK (purple) and Chukchi Sea (orange). Units of LCC and near-surface temperature are % and K, respectively. SH and LH are expressed in W m^{-2}. Bars left and right (up and down) of each symbol indicate the respective standard deviation of the mean PD (FUT-PD) values across models. The numbers in different colors within each subfigure indicate the areal-mean ERA5 values following the same color convention as for the symbols.

the four models over most of the high-latitude regions affected by sea-ice loss. The largest warm-ups are located over areas with largest sea-ice loss, but their magnitudes vary considerably across models: more warming is simulated by FGOALS-f3-L and TaiESM1, and less warming by IPSL-CM6A-LR and NorESM2-LM. Furthermore, models showing the largest reductions in LCC over HB and CS are also those experiencing the largest increases in near-surface temperature. This feature, possibly related to enhanced lower-troposphere vertical mixing in response to the excessive surface warming, is addressed later. In any case, it is worth keeping in mind that these increases in near-surface temperature are expected to result from changes in surface fluxes and not in solar radiation, given that during the season under analysis the sunlight is low or even absent.

4. Mechanisms Related to the Uneven Responses of LCC to Arctic Sea-Ice Loss

In this section, we explore the physical processes responsible for the model divergence in the response of LCC to sea-ice loss. We start comparing aspects of the models' mean PD climatologies and their response to sea-ice loss for each region (Figure 3). We then quantify the simulated variations in the vertical profiles of temperature and moisture over the different regions to explain the disagreements in the response (Figure 4). Results are presented for each region separately.

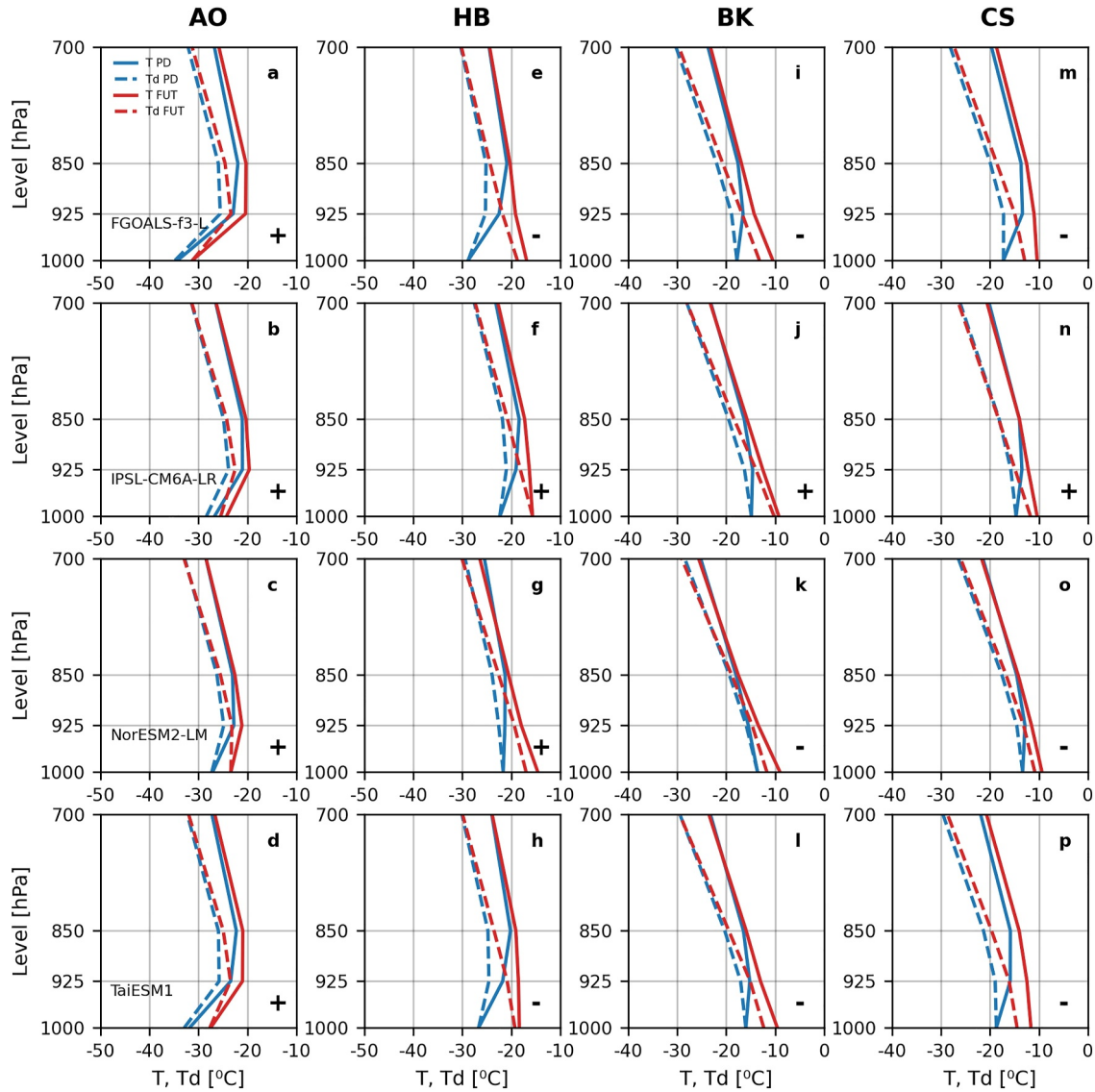

Figure 4. Vertical profiles of dry-bulb and dew-point temperatures (full and dashed lines respectively, in units of °C) between 1,000 and 700 hPa for each model (rows) and over the four regions (columns) for PD (blue) and FUT (red) experiments. The plus (minus) sign in the lower right corner of each figure indicates an increase (decrease) in Low-cloud cover for that given model and that region.

1. *AO*

In terms of LCC (Figure 3a), all models simulate an increase of less than 10% in cloudiness and a net warming of between 2°C and 4°C (Figure 3b). Meanwhile, almost no changes are simulated in the turbulent fluxes over this region (Figures 3c and 3d), suggesting that the simulated variations in LCC over the region are not explained by surface processes but by other mechanisms. An inspection of the simulated variations in the lower-tropospheric circulation (not shown) hints at an intensification of the southerly winds toward AO in most of the models, carrying warmer air into the region (explaining the simulated warming) alongside air masses with higher moisture content driving an increase in water vapor pressure (Figure S3 in Supporting Information S1). A comparison of the PD mean values against those derived from ERA5 highlights a negative bias in simulations of LCC (IPSL-CM6A-LR and NorESM2-LM) and near-surface temperature (all the models) over this region.

Vertical temperature profiles over AO show a strong temperature inversion extending from the surface to 850 hPa (Figures 4a–4d). This inversion is strongest in FGOALS-f3-L and TaiESM1 (Figures 4a–4d), in line with them being the coldest models, and weakens slightly (but is still present) under sea-ice loss. A comparison against

ERA5 data shows that the two colder models overestimate the magnitude of the inversion, while the two others are closer to the reanalysis (Figures S5b, S6a and S6e in Supporting Information S1). In the absence of an effect from surface turbulent fluxes (Figure 3), the weakening of the inversion simulated by the models could be explained by advective processes that shape thermal stratification as discussed previously. Changes on the inversion strength were computed considering the changes on the inversion layer depth between PD and FUT, shown in Figure S7 in Supporting Information S1.

2. *HB*

Noticeable disagreements are found over this region: LCC changes (Figure 3a) are negative in FGOALS-f3-L and TaiESM and positive in IPSL-CM6A-LR and NorESM-LM, in line with the largest spread in LCC as discussed before (Figure 2), but it is once again interesting to note that models associated with larger cloud cover in the PD experiments are also the ones simulating decreased cloudiness in FUT. The opposite holds for models with lower mean PD LCC values. Another remarkable characteristic is that the cloudier models in PD climate are not only the coldest ones (Figure 3b) but also those experiencing the largest warming amounts (and cloud reductions) when sea ice decreases. Changes in turbulent fluxes (Figures 3c and 3d) are largest for both SH and LH in the FGOALS-f3-L model, and little differences are found for the others. As a result, an increase in surface water vapor pressure is simulated by all models and maximized in FGOALS-f3-L (Figure S3 in Supporting Information S1).

The significant loss of sea ice over HB leads to the development of a heat low (Smith et al., 2022). This heat low, which results from the surface warming following sea-ice loss (Figures 4e–4h), fosters an enhancement of the upward motion (not shown) and, consequently, a drop in surface pressure. Interestingly, and despite the noticeable differences in the strength of the temperature inversion across models (Figures S4 and S6 in Supporting Information S1), a complete erosion of the inversion is simulated in all the models in FUT experiments, in line with the almost complete erosion of sea ice over this area.

The surface warming resulting from sea-ice loss, strongest in models with colder PD climate (i.e., FGOALS-f3-L and TaiESM1), leads to noticeable differences in temperature and moisture profiles over HB (Figures 4e–4h). Low-level moisture increases with sea-ice loss in the four models, although the largest absolute values are achieved in the warmer models. In these models, the warm and moist conditions under less sea ice result in less stable conditions, pushing clouds into higher altitude (Figure S7 in Supporting Information S1) due to the increased boundary layer height. NorESM2-LM (Figure S7g in Supporting Information S1) simulates the largest rise in clouds, in line with it already depicting the less stable conditions in the PD climate. The colder models show the maximum cloud cover lifting from the surface to several hundred meters above the ground after sea-ice loss (Figures S7e and S7h in Supporting Information S1). However, the maximum cloud cover is noticeably reduced in both models compared to PD values due to the prevailing effect from the large surface warming that dilutes the low cloud deck within the inversion layer. The changes in temperature and dewpoint profiles as well as the lifting of the cloud deck all suggest enhanced vertical mixing in these models. Consequently, the uneven patterns of variations in the vertical distributions of temperature and moisture explain why the colder models simulate a decrease in cloudiness (disappearance of the low cloud deck within the inversion layer) whereas the warmer models simulate an increase in LCC (lifting of the boundary layer top and deeper ascent within that layer) under sea-ice loss.

3. *BK*

Disagreements on the LCC response to sea-ice loss are also evident here across models, even though not as strongly as over HB. Once again, models with larger LCC in the PD climate are the ones depicting the largest reductions following sea-ice melt (Figure 3a) and the ones characterized by the colder conditions in the PD: FGOALS-f3-L and TaiESM1 (Figure 3b). Comparison against ERA5 suggests smaller biases in terms of near-surface temperature over this region, even though the colder models are still below the ERA5 mean values for the 1979–2008 period. Both turbulent fluxes increase over BK as a response to sea-ice loss, but SH increases slightly more in the colder models, while variations in LH fluxes are overall more similar among models, close to a 100% increase when compared to the PD conditions.

The vertical stratification of temperature is noticeably less stable than over AO and HB (Figures 4i–4l, Figure S6c in Supporting Information S1). In fact, the warmer models IPSL-CM6A-LR and NorESM2-LM are characterized either by a very weak inversion (in the case of the former) or no inversion (in the latter). On the other hand, the

colder models have better-defined inversion layers, albeit with weak magnitudes. These compare overall well with ERA5, which simulates no inversion over the BK region (Figure S5d in Supporting Information S1).

Most of the models simulate a reduction in LCC in response to sea-ice loss. The analysis of the simulated changes in the vertical structures of temperature and moisture (Figure 4) shows that these reductions are explained by the warming of the surface layer and a relatively minor effect from the slight increase in moisture content. The only exception is IPSL-CM6A-LR, which simulates an LCC increase of less than 5% due to a more prominent effect from the lower-troposphere moisture content, which is the largest among the four models.

4. *CS*

Results for this region are overall very similar to those discussed for BK. Once again, the colder models in PD have the strongest inversions over CS (Figures S6d and S5e in Supporting Information S1). However, the warmer models are characterized by an inversion layer which is not only weaker, but also much closer to ERA5. The only model hinting at an increase in LCC is once again IPSL-CM6A-LR and this results from the slightly more humid conditions within the layer 1,000/850 hPa simulated by this model (Figure 4n).

5. Discussion and Conclusions

Recent studies have shown that Arctic sea-ice loss fosters increased LCC between October and March (Jenkins et al., 2024). In this study, we have shown using a set of experiments forced by changes in sea-ice cover that the simulated response of LCC to sea-ice loss is not uniform across models and that it depends on the region under analysis. Over the AO, the effect from sea-ice loss on LCC is indirect as the net reduction of winter sea ice over that region is expected to be marginal in the coming decades. All the models analyzed in this study simulate a future increase in LCC over that region due to changes in the surface pressure field over the subpolar latitudes, which favors warmer and moisture-rich air masses to reach AO. We have also analyzed three regions which are expected to experience significant sea-ice loss in the upcoming decades: the HB, the northern Barents-Kara Sea (BK) and the CS. Over these three regions, the effect from sea-ice loss is direct, and in fact variations in surface fluxes are substantially more important than regional changes in the circulation. We found for BK and CS that most of the models simulate a reduction in LCC under sea-ice loss due to a predominant effect from surface warming and a secondary role of the increase in lower-tropospheric moisture via enhanced evaporation. The only model simulating the opposite pattern (IPSL-CM6A-LR) is in turn characterized by a weaker warming of the lower levels and a higher impact from the moisture gain, leading to a net increase in LCC.

The largest disagreements across models were found over HB, where two models simulate an increase in LCC with sea-ice loss and the two others, a decrease. A detailed inspection of the associated mechanisms showed that the two models simulating reduced LCC are those characterized by the coldest surface conditions in the present-day climate, alongside the highest amount of LCC. When sea ice is reduced, this colder mean state promotes the onset of intense vertical fluxes of sensible heat, leading to a significant warming of the lower troposphere. Therefore, the strong vertical mixing triggered by this excessive warming leads to a sharp increase in lower-tropospheric temperatures as well as to a reduction in moisture content closer to the surface layer, both of which argue for decreasing LCC. On the other hand, models that are warmer in the present-day climate experience a weaker warming when sea ice is reduced. This results in a more prevalent role from the moisture rather than the temperature increase on LCC, which in this case increases.

A comparison between models and ERA5 reanalysis showed that the colder models simulate too strong inversions over all the regions under analysis. Furthermore, the warmer models in the present-day climate not only display more realistic inversion layers but also show very weak or no inversion over the BK region, in agreement with ERA5. As such, these could be potentially giving more trustful information on the fate of LCC under sea-ice loss for the coming decades. However, there are many other forcings that affect the distribution and variability of clouds over high latitudes, and these may vary in a way that could neutralize or even overcompensate those triggered by sea-ice loss alone. Future work in the field should be driven into assessing these, their interplay and the eventual total effect on cloudiness around the Arctic region.

Conflict of Interest

The authors declare no conflicts of interest relevant to this study.

Data Availability Statement

The PAMIP data is available from https://esfg-node.llnl.gov/search/cmip6/. The ERA5 data is available at Hersbach et al. (2023).

Acknowledgments
The authors acknowledge the comments from two anonymous reviewers, which helped improve and clarify the manuscript. This work is part of the Horizon 2021 Polar2MidLat project, funded by the European Union under the Marie Skłodowska-Curie Grant 101061202.

References

Arouf, A., Chepfer, H., Kay, J., L'Ecuyer, T., & Lac, J. (2024). Surface cloud warming increases as late fall Arctic sea ice cover decreases. *Geophysical Research Letters*, *51*(3), e2023GL105805. https://doi.org/10.1029/2023GL105805

Barnes, E., & Screen, J. (2015). The impact of arctic warming on the midlatitude jet-stream: Can it? Has it? Will it? *WIRES Climent Change*, *6*(3), 277–286. https://doi.org/10.1002/wcc.337

Boucher, O., Randall, D., Artaxo, P., Bretherton, C., Feingold, G., Forster, P., et al. (2013). Clouds and aerosols. In T. Stocker, D. Qin, G. Plattner, M. Tignor, S. Allen, J. Boschung, et al. (Eds.), *Climate change 2013: The physical science basis. Contribution of working group I to the fifth assessment report of the intergovernmental panel on climate change* (pp. 571–657). Cambridge University Press. https://doi.org/10.1017/CBO9781107415324.016

Cohen, J., Screen, J., Furtado, J., Barlow, M., Whittleston, D., Coumou, D., et al. (2014). Recent arctic amplification and extreme mid-latitude weather. *Nature Geoscience*, *7*(9), 627–637. https://doi.org/10.1038/ngeo2234

Devasthale, A., Willén, U., Karlsson, K., & Jones, C. (2010). Quantifying the clear-sky temperature inversion frequency and strength over the Arctic Ocean during summer and winter seasons from AIRS profiles. *Atmospheric Chemistry and Physics*, *10*(12), 5565–5572. https://doi.org/10.5194/acp-10-5565-2010

Goosse, H., Kay, J., Armour, K., Bodas-Salcedo, A., Chepfer, H., Docquier, D., et al. (2018). Quantifying climate feedbacks in polar regions. *Nature Communications*, *9*(1), 1919. https://doi.org/10.1038/s41467-018-04173-0

Griesche, H., Barrientos-Velasco, C., Deneke, H., Hünerbein, A., Seifert, P., & Macke, A. (2024). Low-level arctic clouds: A blind zone in our knowledge of the radiation budget. *Atmospheric Chemistry and Physics*, *24*(1), 597–612. https://doi.org/10.5194/acp-24-597-2024

Gryning, S.-E., Batcharova, E., Floors, R., Münkel, C., Skov, H., & Sørensen, L. (2021). Comparison of ERA-5 reanalysis and observed cloud cover in the high arctic. *EMS Annual Meeting*, *2021*, EMS2021-276. https://doi.org/10.5194/ems2021-276

Hall, A. (2004). The role of surface albedo feedback in climate. *Journal of Climate*, *17*(7), 1550–1568. https://doi.org/10.1175/1520-0442(2004)017<1550:TROSAF>2.0.CO;2

Hay, S., Priestley, M., Yu, H., Catto, J., & Screen, J. (2023). The effect of arctic sea-ice loss in extratropical cyclones. *Geophysical Research Letters*, *50*(17), e2023GL102840. https://doi.org/10.1029/2023GL102840

Hersbach, H., Bell, B., Berrisford, P., Biavati, G., Horányi, A., Muñoz Sabater, J., et al. (2023). ERA5 hourly data on pressure levels from 1940 to present [Dataset]. *Copernicus Climate Change Service (C3S) Climate Data Store (CDS)*. https://doi.org/10.24381/cds.bd0915c6

Hersbach, H., Bell, B., Berrisford, P., Hirahara, S., Horányi, A., Muñoz-Sabater, J., et al. (2020). The ERA5 global reanalysis. *Quarterly Journal of the Royal Meteorological Society*, *146*(730), 1999–2049. https://doi.org/10.1002/qj.3803

Jenkins, M., Dai, A., & Deser, C. (2024). Seasonal variations and spatial patterns of arctic cloud changes in association with sea ice loss during 1950-2019 in ERA5. *Journal of Climate*, *37*(2), 735–754. https://doi.org/10.1175/JCLI-D-23-0117.1

Kay, J., & Gettelman, A. (2009). Cloud influence on and response to seasonal arctic sea ice loss. *Journal of Geophysical Research*, *114*(D18), D18204. https://doi.org/10.1029/2009JD011773

Kay, J., L'Ecuyer, T., Chepfer, H., Loeb, N., Morrison, A., & Cesana, G. (2016). Recent advances in arctic cloud and climate research. *Current Climate Change Reports*, *2*(4), 159–169. https://doi.org/10.1007/s40641-016-0051-9

Klein, S., & Neggers, R., & coauthors. (2009). Intercomparison of model simulations of mixed-phase clouds observed during the ARM mixed-phase arctic cloud experiment. Part I: Single layer cloud. *Quarterly Journal of the Royal Meteorological Society*, *135*, 979–1002. https://doi.org/10.1002/qj.416

Li, X., Mace, G., Strong, C., & Krueger, S. (2023). Wintertime cooling of the arctic TOA by low-level clouds. *Geophysical Research Letters*, *50*(17), e2023GL104869. https://doi.org/10.1029/2023GL104869

Liu, Y., & Key, J. (2025). Cold season cloud response to sea ice loss in the arctic. *Journal of Climate*, *38*(1), 347–368. https://doi.org/10.1175/JCLI-D-23-0394.1

Liu, Z., & Schweiger, A. (2024). ICESat-2 shows sea ice leads have little overall effects on the arctic cloudiness in cold months. *Journal of Climate*, *37*(15), 4045–4058. https://doi.org/10.1175/JCLI-D-23-0285.1

Maillard, J., Ravetta, F., Raut, J.-C., Mariage, V., & Pelon, J. (2021). Characterisation and surface radiative impact of arctic low clouds from the IAOOS field experiment. *Atmospheric Chemistry and Physics*, *21*(5), 4079–4101. https://doi.org/10.5194/acp-21-4079-2021

Manabe, S., & Stouffer, R. (1994). Multiple-century response of a coupled ocean-atmosphere model to an increase of atmospheric carbon dioxide. *Journal of Climate*, *7*(1), 5–23. https://doi.org/10.1175/1520-0442(1994)007<0005:MCROAC>2.0.CO;2

May, R., Goebbert, K., Thielen, J., Leeman, J., Camron, M., Buick, Z., et al. (2022). MetPy: A meteorological python library for data analysis and visualization. *Bulletin America Meteorology Social*, *103*(10), E2273–E2284. https://doi.org/10.1175/BAMS-D-21-0125.1

Neggers, R., Siebesma, A., & Heus, T. (2012). Continuous single-column model evaluation at a permanent meteorological supersite. *Bulletin America Meteorology Social*, *93*(9), 1389–1400. https://doi.org/10.1175/BAMS-D-11-00162.1

Philipp, D., Stengel, M., & Ahrens, B. (2020). Analyzing the arctic feedback mechanism between sea ice and low-level clouds using 34 years of satellite observations. *Journal of Climate*, *33*(17), 7479–7501. https://doi.org/10.1175/JCLI-D-19-0895.1

Pithan, F., Medeiros, B., & Mauritsen, T. (2014). Mixed-phase clouds cause climate model biases in arctic wintertime temperature inversions. *Climate Dynamics*, *43*(1–2), 289–303. https://doi.org/10.1007/s00382-013-1964-9

Rayner, N., Parker, D., Horton, E., Folland, C., Alexander, L., Rowell, D., & Kaplan, A. (2003). Global analyses of sea surface temperature, sea ice, and night marine air temperature since the late nineteenth century. *Journal of Geophysical Research*, *108*(D14), 4407. https://doi.org/10.1029/2002JD002670

Screen, J., Deser, C., & Simmonds, I. (2012). Local and remote controls on observed arctic warming. *Geophysical Research Letters*, *39*(10), L10709. https://doi.org/10.1029/2012GL051598

Screen, J., Eade, R., Smith, D., Thompson, S., & Yu, H. (2022). Net equatorward shift of the jet streams when the contribution from sea-ice loss is constrained by observed eddy feedback. *Geophysical Research Letters*, *49*(23), e2022GL100523. https://doi.org/10.1029/2022GL100523

Screen, J., & Simmonds, I. (2010). The central role of diminishing sea ice in recent arctic temperature amplification. *Nature*, *464*(7293), 1334–1337. https://doi.org/10.1038/nature09051

Sedlar, J., & Tjernström, M. (2009). Stratiform cloud-inversion characterization during the arctic melt season. *Boundary-Layer Met*, *132*, 455–474. https://doi.org/10.1007/s10546-009-9407-1

Sledd, A., & L'Ecuyer, T. (2019). How much do clouds mask the impacts of arctic sea ice and snow cover variations? Different perspectives from observations and reanalyses. *Atmosphere*, *10*(1), 12. https://doi.org/10.3390/atmos10010012

Sledd, A., & L'Ecuyer, T. (2021). A cloudier picture of ice-albedo feedback in CMIP6 models. *Frontiers in Earth Science*, *9*, 769844. https://doi.org/10.3389/feart.2021.769844

Smith, D., Eade, R., Andrews, M., Ayres, H., Clark, A., Chripko, S., et al. (2022). Robust but weak winter atmospheric circulation response to future arctic sea ice loss. *Nature Communications*, *123*(1), 727. https://doi.org/10.1038/s41467-022-28283-y

Smith, D., Screen, J., Deser, C., Cohen, J., Fyfe, J., García-Serrano, J., et al. (2019). The polar amplification model intercomparison project (PAMIP) contribution to CMIP6: Investigating the causes and consequences of polar amplification. *Geoscientific Model Development*, *12*(3), 1139–1164. https://doi.org/10.5194/gmd-12-1139-2019

Solomon, A., Morrison, H., Persson, O., Shupe, M., & Bao, J.-W. (2009). Investigation of microphysical parameterizations of snow and ice in arctic clouds during M-PACE through model-observation comparisons. *Monthly Weather Review*, *137*(9), 3110–3128. https://doi.org/10.1175/2009MWR2688.1

Tjernström, C., Leck, P., Persson, G., Jensen, M., Oncley, S., & Targino, A. (2004). The summertime arctic atmosphere: Meteorological measurements during the Arctic Ocean experiment 2001. *Bulletin America Meteorology Social*, *85*, 1305–1322. https://doi.org/10.1175/BAMS-85-9-1305

Tjernström, M., Sedlar, J., & Shupe, M. (2008). How well do regional climate models reproduce radiation and clouds in the arctic? An evaluation of ARCMIP simulations. *Journal of Applied Meteorology and Climatology*, *47*(9), 2405–2422. https://doi.org/10.1175/2008JAMC1845.1

Wang, D., Guo, J., Chen, A., Bian, L., Ding, M., Liu, L., et al. (2020). Temperature inversion and clouds over the Arctic Ocean observed by the 5th Chinese national arctic research expedition. *Journal of Geophysical Research: Atmospheres*, *125*(13), e2019JD032136. https://doi.org/10.1029/2019JD032136

Wilks, D. (2006). On "field significance" and the false discovery rate. *Journal of Applied Meteorology and Climatology*, *45*(9), 1181–1189. https://doi.org/10.1175/JAM2404.1

Ye, K., Woollings, T., Sparrow, S., Watson, P., & Screen, J. (2024). Response of winter climate and extreme weather to projected arctic sea-ice loss in very large-ensemble climate model simulations. *npj Clim. Atmos. Sci.*, *7*(1), 20. https://doi.org/10.1038/s41612-023-00562-5

Zhang, L., Ding, M., Dou, T., Huang, Y., Lv, J., & Xiao, C. (2021). The shallowing surface temperature inversions in the arctic. *Journal of Climate*, *34*(10), 4159–4168. https://doi.org/10.1175/JCLI-D-20-0621.1

Zhang, Y., Seidel, D., Golaz, J.-C., Deser, C., & Tomas, R. (2011). Climatological characteristics of arctic and antarctic surface-based inversions. *Journal of Climate*, *24*(19), 5167–5186. https://doi.org/10.1175/2011JCLI4004.1